RESEARCH ARTICLE

ADVANCED SENSOR RESEARCH Open Access

www.advsensorres.com

An Untethered Heart Rhythm Monitoring System with Automated AI-Based Arrhythmia Detection for Closed-Loop Experimental Application

*Shanliang Deng, Bram L den Ouden, Tim De Coster, Cindy I Bart, Wilhelmina H Bax, René H Poelma, Antoine AF de Vries, Guo Qi Zhang, Vincent Portero, and Daniël A Pijnappels**

The heart produces bioelectrical signals, which can be measured as an electrocardiogram (ECG) for the detection of rhythm disturbances. Rapid and precise detection of these arrhythmias is crucial for their termination by closed-looped therapeutic interventions to counteract detrimental effects. However, there is a current lack of such systems tailored for experimental cardiovascular applications. This hampers not only in-depth mechanistic studies but also translational testing of new therapeutic strategies, especially in an untethered manner in awake animal models. To break new ground, recent advances to develop a non-invasive AI-supported heart rhythm monitoring system for untethered automated arrhythmia detection in a continuous manner is combined. This system is housed in a lightweight jacket for mobile use and includes an on-skin ECG sensor, a low-power microprocessor unit, a massive data storage unit, and a power-management system. By implementing a novel hybrid algorithm based on so-called heart rate (R-R) variability and a case-specific AI model, 100% sensitivity and 95% specificity is achieved in detecting atrial arrhythmias within 2 s upon initiation in adult rats. Thereby, the novel system sets the stage for advanced mechanistic studies and therapeutic testing, including closed-loop applications aiming for the termination of a broad range of atrial arrhythmias.

1. Introduction

Living organs produce biosignals, which can be detected and used to monitor the organ's health. In the case of the heart, one of the biosignals generated by the organ is bioelectricity, which can be measured using the electrocardiogram (ECG) technique to reveal cardiac rhythm.[1] ECGs can be used for the detection and diagnosis of various cardiac rhythm disorders, such as atrial arrhythmias. Atrial arrhythmias are often characterized by faster heart rates that are either regular (atrial flutter – AFL) or irregular (atrial fibrillation – AF).[2] Animal models, particularly rats, are widely used in experimental laboratories to investigate the mechanisms and treatment of atrial arrhythmias. As such disorders are not only detrimental but also progressive in nature, there is a clear impetus to detect and terminate them as quickly as possible.[3] This requires continuous and precise monitoring of cardiac rhythm to enable immediate and accurate detection of atrial arrhythmias, irrespective of their specific features such as duration and (ir)regularity. In an attempt to meet these criteria, implantable telemetry devices have been widely adopted for continuous monitoring of cardiac electrical activity.[4] However, these commercially available ECG telemetry systems require surgical intervention for implantation of the device into the rat body, which not only causes animal harm but can also lead to unexpected physical and psychological influences on heart rhythm.[5] Moreover, these devices can only operate for a certain amount of time and, therefore, require additional surgical interventions in case of prolonged monitoring.[6] Hence, these systems are less suited for continuous monitoring over extended periods of time, which is needed given the timescale on which arrhythmias develop, progress and exert their detrimental effects. On top of the disadvantages mentioned above, current telemetry systems need external receiving devices for real-time visualization and recording of the ECG data. Therefore, a separate computer with signal processing software is required to recognize abnormal cardiac activities such as atrial arrhythmias. In

S. Deng, B. L den Ouden, T. De Coster, C. I Bart, W. H Bax, A. A. de Vries, V. Portero, D. A Pijnappels
Laboratory of Experimental Cardiology
Department of Cardiology
Heart Lung Center Leiden
Leiden University Medical Center
Leiden 2333 ZA, Netherlands
E-mail: d.a.pijnappels@lumc.nl

S. Deng, B. L den Ouden, R. H Poelma, G. Q. Zhang
Department of Microelectronics
Delft University of Technology
Delft 2628 CD, Netherlands

The ORCID identification number(s) for the author(s) of this article can be found under https://doi.org/10.1002/adsr.202400057

DOI: 10.1002/adsr.202400057

most animal facilities, setting up such a complex system is not compatible with long-term monitoring due to animal facility constraints.

A stand-alone, untethered miniaturized device allowing real-time atrial arrhythmia detection could offer a solution to these problems and thereby improve current research possibilities and unlock new ones. Such a device should have a minimal weight and be able to measure ECGs in rats in a non-invasive manner. Then, a processor integrated into the device should allow real-time analysis and wireless transmission of the ECG, reporting atrial arrhythmias events when they occur. Also, all the ECG data and atrial arrhythmias events should be stored in a large storage unit for later inspection of the data.

The most common method to detect atrial arrhythmias is based on the irregularity of the so-called R-R interval of the ECG signal, which works well in most AF cases.[7] However, a subset of atrial arrhythmia cases, like AFL, present a stable heart rhythm, precluding their detection by R-R detection algorithms.[8] With the development of artificial intelligence (AI), new detection algorithms based on deep learning have been developed, enabling the detection of all types of atrial arrhythmias in humans.[9] The development of these AI detection algorithms required training using large human ECG databases,[10] which are non-existent for laboratory animals, making a similar strategy not feasible for laboratory animal research. Additionally, these new algorithms require high calculation power beyond that of a stand-alone miniaturized system's ability, making this technology inapplicable to small animals such as rats.

In order to still exploit the powerful features of AI in arrhythmia detection, an alternative approach could be adopted by using case-specific AI models. Such a strategy would consist of training a "personal" AI model for each rat individually based on short episodes of ECG recordings. This approach would simultaneously decrease the model size and calculation power needed for training, making the use of AI technology compatible with a stand-alone miniaturized system.[11]

In this manuscript, we have explored and realized all of the above to present a non-invasive real-time on-chip automatic atrial arrhythmia detection system for rats. The whole system is miniaturized and embedded in a spandex jacket designed for rats. Hardware-wise, this system contains an ECG amplifier, a non-invasive stretchable electrode, an ESP32 low-power processor, a removable large data storage unit, and a rechargeable battery. In terms of software, a hybrid algorithm consisting of an improved R-R detection algorithm and a case-specific AI algorithm is implemented in the ESP32 processor to detect atrial arrhythmias by analyzing the ECG signal in real time. Collectively, the results from our study create a basis for next-generation biomedical devices addressing unmet needs in biosignal processing for pre-clinical cardiovascular research including closed-looped therapeutic interventions.

2. Results and Discussion

2.1. ECG Measurement

Our atrial arrhythmia detection system (**Figure** 1A) was able to sample ECG signals and automatically detect R-wave peaks as shown on the ECG traces (Figure 1B) recorded in an anesthetized rat. The dots on top of the trace show the on-chip automated peak detection. Our system also allowed the visualization of other ECG waves (i.e., the QRS complex, T wave, and P wave) similar to conventional PowerLab ECG recordings. The main function of our device is to detect atrial arrhythmias rather than measure accurate electrophysiological values. No absolute biopotential values were needed for AI and R-R detection algorithms. Therefore, normalized ECG signals were used throughout this study.

To further validate the system, we pharmacologically changed the heart rate by intraperitoneal injections of either isoprenaline or carbachol. This led, within 1 min, to a 30 ms decrease (from 357 to 434 bpm) or a 20 ms increase (from 357 to 319 bpm) in R-R interval, respectively, as shown in Figure 1C,D. Comparison of the R-R interval measured by our system and by PowerLab (Figure 1E,F) showed a high correlation between both ECG systems (R^2 = 99.8). Our atrial arrhythmia detection algorithm reported sinus rhythm (SR) after pharmacological induction of both faster and slower heart rates, confirming that physiological heart rate changes should not lead to false positive detection of atrial arrhythmias (evaluated only with the R-R algorithm).

2.2. Atrial Arrhythmia Detection

The data stored on the microSD card by our system was extracted and analyzed in each experiment. Atrial arrhythmias were successfully generated in 5 rats (108 episodes of atrial arrhythmia induced by 314 rounds of burst pacing (BP)). The duration distribution of these arrhythmias is shown in Figure S5A. Almost half of the induced arrhythmias lasted less than 5 s and the average duration of all arrhythmias was 12.3 s. The detection results during BP were ignored. The result of detection can be categorized into true positive (TP, arrhythmias detected), true negative (TN, SR detected), false positive (FP, SR detected as arrhythmias), and false negative (FN, arrhythmias not detected).[12]

In the case of AF, as shown in **Figure** 2A, the R-R and AI algorithms both detected the arrhythmia. The R-R algorithm detected the arrhythmia 3 s after initiation because it requires 10 peaks to confirm or deny AF detection. This also explains the observed delay in detecting the cessation of AF. The AI algorithm, on the other hand, provided a much faster indication (i.e., within 1 s) of the presence or absence of AF.

In some rare cases of AFL, as shown in Figure 2B, the R-R interval varied less than 10% compared to the baseline. Thus, even our improved R-R algorithm was unable to detect the arrhythmia, while the AI algorithm could still detect the AFL within a similarly short time period after its initiation as in the case of AF. The logical OR of the result (R-R: FN, AI: TP) was true. Thus, this AFL event was reported as a true positive case by the hybrid algorithm.

Figure 2C shows a typical example of a 1 min continuous detection result containing 6 BP events and 3 spontaneously terminating arrhythmia episodes. Both algorithms reported SR when no arrhythmia was induced and detected all 3 arrhythmia episodes. In most cases, the AI algorithm could give an immediate indication within 1 s, while the R-R algorithm detected the arrhythmia with an average delay of 2 s. By applying the hybrid algorithm, the system could take advantage of the AI algorithm to reach a shorter detection time.

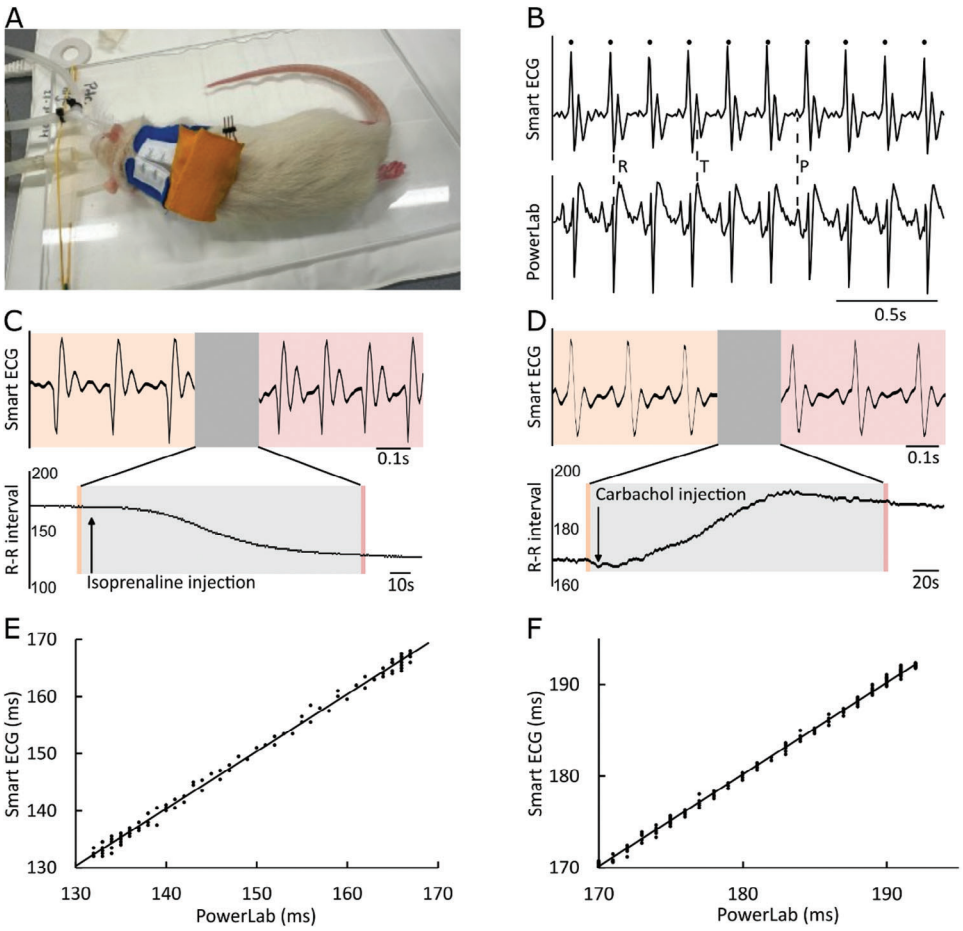

Figure 1. ECG recording and automated R wave detection in rats using our system. A) Our system in a compact pocket attached with Velcro (orange) to the rat jacket (blue) at the back of the animal; B) ECG signal comparison between our system versus the PowerLab bio amplifier (Dot on top of the trace indicates the on-chip peak detection); C) Monitoring of R-R interval decrease after injection of isoprenaline. Episodes in orange and red background show the ECG before and after drug administration, respectively; D) Monitoring of heart rate decrease after injection of carbachol. Episodes in orange and red background show the ECG before and after drug administration, respectively; Correlation between our system and PowerLab (LabChart calculated) R-R interval measurements during isoprenaline E) and carbachol injection F).

Among all the arrhythmias induced, the R-R algorithm reaches an overall detection sensitivity (TP/[TP+FN]) of 79.6% and specificity (TN/[TP+FN]) of 98.5%, with an average detection time of 2.1 s as shown in the red zone of Figure 2D. The AI algorithm had an overall sensitivity of 84.2% and a specificity of 97%, with an average detection time of 0.75 s as indicated by the yellow zone in Figure 2D. Interestingly, the AI algorithm showed a 25% higher sensitivity to detect short arrhythmias (<3 s) than the R-R algorithm while the R-R algorithm had a ≈10% higher sensitivity to detect longer arrhythmias (>3 s) than short ones, as illustrated in Figure 2E. The hybrid algorithm could combine the advantage of the AI algorithm for short arrhythmia detection and the R-R algorithm for the detection of longer arrhythmias to reach a high sensitivity for arrhythmias of all durations. Overall, the hybrid algorithm reached a sensitivity of 96.3% and a specificity of 95.5%, with an average detection time of 0.85 s. The detection result of the hybrid algorithm is shown as the blue line in Figure 2D,E. Compared to individual R-R and AI algorithms, the hybrid algorithm had a higher sensitivity across all arrhythmias durations and reached 100% sensitivity for arrhythmias longer than 2 s.

3. Conclusion

In this paper, we present a non-invasive system enabling continuous in vivo heart rhythm monitoring and atrial arrhythmia detection in a fully untethered and automated manner. By applying our system to adult rats, we demonstrate its ability to rapidly detect atrial arrhythmias with high sensitivity. These results set the stage for long-term investigative studies by continuously monitoring heart rhythm in freely walking animals without surgery, thereby creating ample freedom to replace, adjust and customize the system components, like the battery.

Compared to traditional atrial arrhythmias detection methods, our system equipped with an R-R- interval and AI-based hybrid atrial arrhythmias detection algorithm, can detect a wide range of atrial arrhythmias, including AF and AFL. Moreover, the algorithm has a high sensitivity to detect arrhythmias of different durations, including extremely short ones.

Our case-specific AI algorithm is the core component of the hybrid algorithm. Instead of collecting a big dataset of rat ECGs to train a generic model, the case-specific AI algorithm

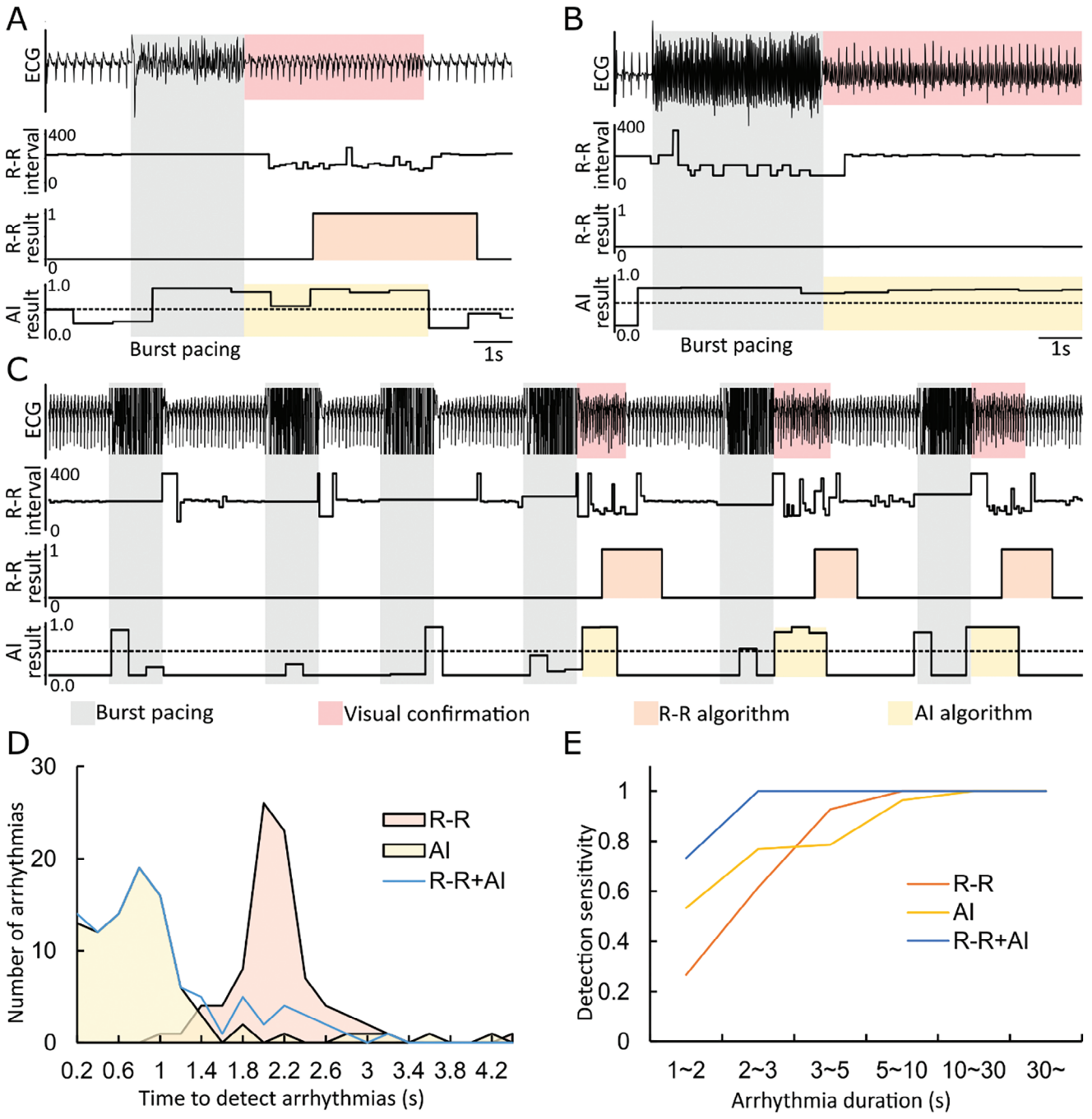

Figure 2. Atrial arrhythmia detection results of our system. A–C) Atrial arrhythmia detection results generated by R-R and AI algorithms. The grey zones across all traces indicate arrhythmia induction by BP, the red zones represent arrhythmias confirmed by manual inspection, the orange zones show the detection result of the R-R algorithm, and the yellow zones show the result of the AI algorithm (0: SR, 1: Atrial arrhythmia); A) Detection result of induced AF; B) Detection result of induced AFL; C) Detection result for 1 min recording; D) Times required for the different algorithms to detect atrial arrhythmia. The X-axis indicates the time to detect an atrial arrhythmia while the Y-axis shows the number of arrhythmias detected in consecutive 0.2 s time periods; E) Atrial arrhythmia detection sensitivity for the different algorithms as a function of arrhythmia duration. The X-axis indicates the duration of atrial arrhythmias, whereas the Y-axis shows the sensitivity to detect atrial arrhythmia of different duration.

drastically decreases the amount of data needed for AI training while maintaining high accuracy by using data sampled from the same rat to train its own model. As a consequence, our device benefits from the advantages offered by AI while presenting a low processing demand compatible with a stand-alone miniaturized system's ability for ambulatory use in rats. In long-term applications, the case-specific AI model could be retrained and easily re-uploaded in case false positive or negative events were be discovered by visual inspection. Such a strategy would allow the sensitivity of the algorithm to be further improved.

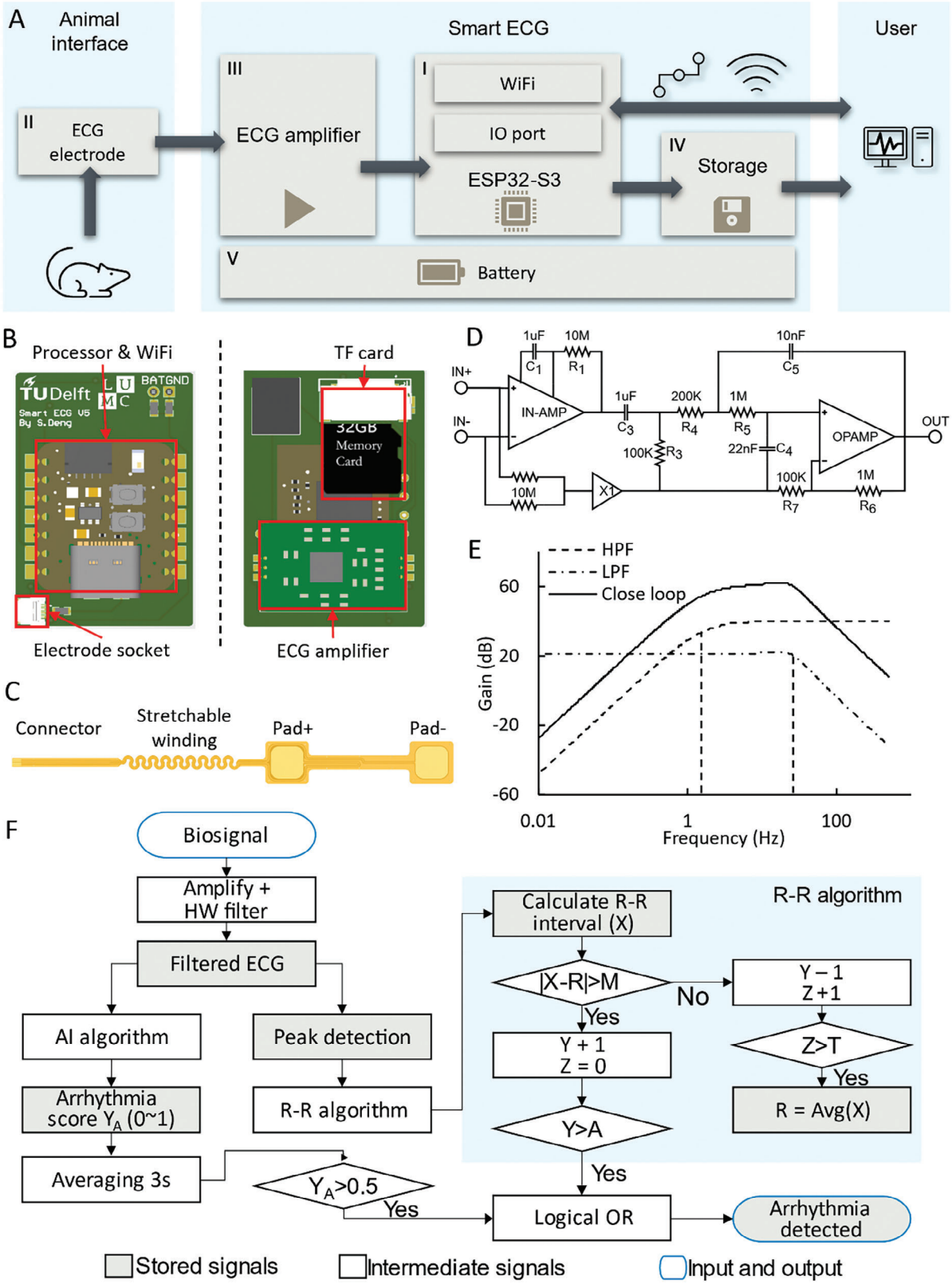

Figure 3. Hardware and software description of the system. A) System diagram of the system; B) Top (left) and bottom view (right) of the hardware module; C) The on-skin flexible electrode for bioelectrical signal recording; D) Peripheral circuit configuration of AD8232 for the ECG amplifier; E) Transfer function of the ECG amplifier; F) Flow chart of the atrial arrhythmia detection algorithm.

Since our system is able to perform fast and accurate detection of atrial arrhythmias in an ambulatory setting, it could be integrated into closed-loop systems to restore normal rhythm through swift intervention. Such closed-loop applications are especially relevant for determining the therapeutic and translational potential of novel strategies for acute arrhythmia termination in awake animals, such as low-voltage multi-pulse therapy,[13] optogenetics,[14] and chemogenetics.[15] Determining this potential in an ambulatory setting is so relevant because it is largely unknown due to the previous absence of systems enabling such investigation. This could provide unique opportunities to prevent or reverse the gradual deterioration of cardiac function caused by the natural progression of AF.[16]

4. Experimental Section

System Hardware Design: The system hardware contains five main parts (**Figure 3A**). The core of this system is an ESP32-S3 (Figure 3A–I) dual-core processor running at 160 MHz clock frequency, located on the top side of the module. This processor serves four functions: reading ECG values using a built-in analog-to-digital converter (ADC), processing ECG data, storing data, and wireless communication. The average power consumption of the processor was 49 mA without real-time wireless streaming, which could consume up to 200 mA. The second part was a flexible body surface electrode (Figure 3A-II,C), which was designed to be placed on the chest of the rat, presenting a flexible structure to avoid discomfort in freely walking animals. The electrode was connected to the ECG amplifier via a flexible printed cable connector. The ECG amplifier (Figure 3A-III) was a modular printed circuit board (PCB) located at the backside of the module, which filters out and amplifies the ECG signal for ADC to read (circuit and transfer function shown in Figure 3D,E). All the ECG data and analysis results were stored on a removable 32 GB micro SD card (Figure 3A-IV), which allows for 1017 h of recording (8 KB s^{-1}). The whole system was powered by a battery management system containing a lightweight removable lithium battery (Figure 3A-V) with a capacity of 200 mAh, allowing 4 h of continuous operation without streaming. For research applications in which discrete recordings would suffice, the processor could be put in deep sleep mode in between recordings to consume as little as 8 µA. This greatly extends the battery lifetime of the device and allows for longer follow-up investigations without human interaction with the animals. All parts in this system were modular, scalable and designed for easy replacement and integrated on a single PCB, as shown in Figures 3B and S1A,B (for PCB design and size, see Figure S4B). To enhance the functionality and research potential of this system, it was tailored and housed in a wearable jacket for the adult rat (Lomir Biomedical). Details about the surface electrode and ECG amplifier are described in the Supporting Information.

Design of R-R Interval-Based Atrial Arrhythmia Detection Algorithm: Commercial atrial arrhythmia detection algorithms, which commonly use the standard deviation of R-R interval variation as an indication, were unable to detect AFL in most cases.[8] This was because AFL had a relatively stable R-R interval as compared to AF. Therefore, AFL's R-R interval standard deviation can appear similar to the one observed in sinus rhythm (SR). Here, an improved atrial arrhythmia detection algorithm (hereafter named R-R algorithm) is introduced, illustrated in Figure 3F, which can also detect AFL using the accumulated R-R interval error as an indication. Details about the R-R algorithm are described in the Supporting Information.

Design of Case-Specific AI-Based Atrial Arrhythmia Algorithm: The case-specific AI algorithm (hereafter named AI algorithm) was built using TensorFlow Convolutional neural network (CNN), the layer configuration of which is shown in Table S1 (Illustrated in Figure S3). This model is meant to train with a limited amount of data in a short time during the experiment. The final size of this model is 12.1 kilobytes, which is small enough to deploy on the ESP32 microprocessor used in the detection device.

The input for this CNN is an array of 200 points, which equals 1 s of ECG data (200 Hz sampling rate). By examining the input ECG data, aside from SR (Figure S2A) and AF (Figure S2C), some events of stable AFL were recorded (Figure S2E). The flutter wave (F wave) in AFL patterns is similar to the noise coupled to the SR in the time domain, which causes false negative arrhythmia detection by the AI algorithm, especially when the training data set is limited. However, in the frequency domain, the noise in the signal clearly differs between SR, AF, and AFL in a frequency-dependent manner. For SR, the heart rate frequency and its harmonics are dominant in the frequency spectrum (Figure S2B), while for AF (Figure S2E) and AFL (Figure S2F), the frequency spectrum of F waves is distributed over all frequencies, causing less clear harmonics. Thus, instead of directly feeding the AI with the ECG signal, it is fed with the Fast Fourier Transforms of the ECG traces in order to enhance the atrial arrhythmia detection sensitivity of the AI algorithm.

In order to train the case-specific AI model to detect atrial arrhythmias, a recording lasting at least 1 minute (60 samples) for both SR and atrial arrhythmias is needed for each rat. The training of the model takes ≈30 s by using an NVIDIA GeForce GTX 1660 Ti graphics card with a training accuracy above 99.5%. The model is then wirelessly transferred to the ESP32 to detect atrial arrhythmias. The AI model generates results every second with a value comprised between 0 and 1 for SR and atrial arrhythmia detection, respectively. By averaging these values over 3 s, a score above 0.5 indicates an ongoing atrial arrhythmia.

Hybrid Algorithm Design: A hybrid algorithm was created to achieve higher atrial arrhythmias detection sensitivity by combining the two algorithms (i.e., the R-R and AI algorithms) mentioned above. The atrial arrhythmias were determined by taking the logical "OR" from the detection result of both algorithms, meaning the hybrid algorithm reports positive as long as one algorithm detects an atrial arrhythmia, and reports negative if both algorithms detect SR. The full flowchart of atrial arrhythmias detection is shown in Figure 3F, with signals highlighted in grey background stored in the micro-SD card for analysis.

Animal Experiment: All animal experiments were approved by the Animal Experiments Committee of Leiden University Medical Center (AVD11600202216629) and conformed to EU Directive 2010/63. This study was conducted with the approval of the institutional review board of the Leiden University Medical Center (PE.16629.01.001).

Supporting Information

Supporting Information is available from the Wiley Online Library or from the author.

Acknowledgements

V.P. and D.A.P. jointly directed this project. This research was supported by the Health Technology program TU Delft and LUMC [20-2602 MEK/MK] to D.A.P. and R.H.P. Additional support was provided by the European Research Council (Consolidator grant 101044831 to D.A.P).

Conflict of Interest

The authors declare no conflict of interest.

Data Availability Statement

The data that support the findings of this study are available from the corresponding author upon reasonable request.

Keywords

artificial intelligence, arrhythmia detection, electrocardiography, non-invasive sensing, on-chip processing

Received: April 17, 2024
Revised: July 3, 2024
Published online: July 31, 2024

[1] W. Einthoven, *Pflügers Archiv European Journal of Physiology* **1895**, *60*, 101.
[2] G. Hindricks, T. Potpara, N. Dagres, E. Arbelo, J. J. Bax, C. Blomstrom-Lundqvist, G. Boriani, M. Castella, G. A. Dan, P. E. Dilaveris, L. Fauchier, G. Filippatos, J. M. Kalman, M. La Meir, D. A. Lane, J. P. Lebeau, M. Lettino, G. Y. H. Lip, F. J. Pinto, G. N. Thomas, M. Valgimigli, I. C. Van Gelder, B. P. Van Putte, C. L. Watkins, *Eur. Heart J.* **2021**, *42*, 373.
[3] Y. C. Chen, A. Voskoboinik, A. Gerche, T. H. Marwick, J. R. McMullen, *J Am Coll Cardiol* **2021**, *77*, 2846.
[4] a) J. A. Segreti, J. S. Polakowski, E. A. Blomme, A. J. King, *J. Pharmacol. Toxicol. Methods* **2016**, *79*, 23; b) S. Eftekhari, C. S. J. Westgate, K. P. Johansen, S. R. Bruun, R. H. Jensen, *Fluids and Barriers of the CNS* **2020**, *17*, 39.
[5] S. Kumstel, P. Vasudevan, R. Palme, X. Zhang, E. H. U. Wendt, R. David, B. Vollmar, D. Zechner, *Journal of Advanced Research* **2020**, *21*, 35.
[6] a) C. Gallet, B. Chapuis, V. Oréa, A. Scridon, C. Barrès, P. Chevalier, C. Julien, *Cardiovascular Engineering and Technology* **2013**, *4*, 535; b) S. Rossi, I. Fortunati, L. Carnevali, S. Baruffi, F. Mastorci, M. Trombini, A. Sgoifo, D. Corradi, S. Callegari, M. Miragoli, E. Macchi, *PLoS One* **2014**, *9*, e112697.
[7] a) M. R. Gold, D. A. Theuns, B. P. Knight, J. L. Sturdivant, R. Sanghera, K. A. Ellenbogen, M. A. Wood, M. C. Burke, *Journal of cardiovascular electrophysiology* **2012**, *23*, 359; b) S. Dash, K. Chon, S. Lu, E. Raeder, *Ann. Biomed. Eng.* **2009**, *37*, 1701.
[8] P. N. Jensen, K. Johnson, J. Floyd, S. R. Heckbert, R. Carnahan, S. Dublin, *Pharmacoepidemiol Drug Saf* **2012**, *21*, 141.
[9] a) U. R. Acharya, S. L. Oh, Y. Hagiwara, J. H. Tan, M. Adam, A. Gertych, R. S. Tan, *Comput. Biol. Med.* **2017**, *89*, 389,; b) J. L. Isaksen, M. Baumert, A. N. L. Hermans, M. Maleckar, D. Linz, *Herzschrittmacherther Elektrophysiol* **2022**, *33*, 34.
[10] I. Matias, N. Garcia, S. Pirbhulal, V. Felizardo, N. Pombo, H. Zacarias, M. Sousa, E. Zdravevski, *Computer Science Review* **2021**, *39*, 100334.
[11] S. Kiranyaz, T. Ince, O. Abdeljaber, O. Avci, M. Gabbouj, In *ICASSP 2019-2019 IEEE International Conference on Acoustics, Speech and Signal Processing* IEEE, New York, **2019**, 8360.
[12] N. Larburu, T. Lopetegi, I. Romero, In *Computing in Cardiology* IEEE, New York, **2011**, 265.
[13] F. S. Ng, O. Toman, J. Petru, P. Peichl, R. A. Winkle, V. Y. Reddy, P. Neuzil, R. H. Mead, N. A. Qureshi, Z. I. Whinnett, D. W. Bourn, M. B. Shelton, J. Kautzner, A. D. Sharma, M. Hocini, M. Haissaguerre, N. S. Peters, I. R. Efimov, *JACC Clin Electrophysiol* **2021**, *7*, 988.
[14] E. C. Nyns, R. H. Poelma, L. Volkers, J. J. Plomp, C. I. Bart, A. M. Kip, T. J. Van Brakel, K. Zeppenfeld, M. J. Schalij, G. Q. Zhang, *Sci. Transl. Med.* **2019**, *11*, 6447.
[15] a) Y. Wexler, M. Ghiringhelli, N. Shaheen, S. Glatstein, I. Huber, O. Edri, Y. Abboud, M. Landesberg, D. Shiff, G. Arbel, L. Gepstein, *Circ. Res.* **2023**, *132*, 645; b) V. Portero, S. Deng, G. J. J. Boink, G. Q. Zhang, A. De Vries, D. A. Pijnappels, *J. Intern. Med.* **2023**, *295*, 126.
[16] T. F. Deering, J. A. Reiffel, A. J. Solomon, K. P. Tamirisa, *Am. J. Cardiol.* **2023**, *205*, S10.